Atomic Wave Diffraction and Interference Using Temporal Slits

Pascal Szriftgiser, David Guéry-Odelin, Markus Arndt, and Jean Dalibard
Laboratoire Kastler Brossel, 24 rue Lhomond, 75005 Paris, France*
(Received 26 February 1996)

We measure the energy distribution of a slow Cesium atomic beam when it is chopped into a short pulse and we find results which agree well with the time-energy uncertainty principle. The chopper consists in an atomic mirror formed by a laser evanescent wave whose intensity is pulsed. We use the temporally diffracted beam to design a Young-slit-type interferometer, in which the interfering paths consist of atomic trajectories bouncing at two different times on the mirror. By changing the mirror intensity, we can scan the atomic phase difference between the two arms. [S0031-9007(96)00519-4]

PACS numbers: 03.75.Dg, 32.80.Pj, 42.50.Vk

When a beam of particles with a well defined energy is chopped into a short pulse, the outcoming energy distribution is broadened according to the time-energy uncertainty relation. This effect is very well known for photons, and it is at the basis of spectroscopy with ultrashort pulses of light. For matter waves, the phenomenon of diffraction by a time slit has been studied theoretically by several authors [1]. Its observation constitutes a test of time-dependent quantum mechanics, while usual diffraction phenomena can be described using the stationary formulation of the Schrödinger equation.

We report here the observation of this temporal diffraction effect for de Broglie atomic waves, and we show that our results are in good agreement with the quantum mechanics prediction. We also use the coherence of the diffracted pulse to realize a Young interferometer using temporal slits. This interferometer is a very flexible device in which the temporal positions of the diffracting slits can be adjusted freely by programming the desired sequence. It corresponds to a "de Broglie interferometer," in which the internal atomic state is the same in the two paths [2,3]. This has to be contrasted with "atomic states interferometers" such that the interfering paths involve two orthogonal internal states α and β, and where the beam splitters usually consist of a resonant interaction between the α-β transition [4]. As we show below, our experimental scheme involves atoms approaching close to a dielectric surface, and this interferometer can provide an efficient way to measure the resulting van der Waals interaction.

Our source is a magneto-optical trap (MOT) of cesium atoms. It is released at time $t = 0$ above an atomic mirror formed with an evanescent laser wave propagating at the surface of a dielectric [5]. The laser wave can be turned off on the microsecond scale, in which case the atoms stick to the dielectric surface instead of bouncing elastically. We first select atoms with a well defined total (kinetic + potential) energy using a sequence of two bounces (Fig. 1), generated by chopping the atomic mirror *on* for two short pulses P_1 and P_2; these pulses are, respectively, centered at time $T = 25$ ms and $3T$, with a variable width τ. From classical mechanics, one would expect after P_2 a triangular energy distribution centered on $E_0 = mg^2T^2/2 = 10h$ MHz (m is the atomic mass and $g = 9.81\ \mathrm{m/s^2}$), with a full width at half maximum (FWHM) $\Delta E_{\mathrm{cl}} = E_0\tau/T$. This prediction has to be compared with the typical width $\Delta E_{\mathrm{Qu}} = h/\tau$ of the sinc-shape energy distribution obtained after the diffraction of a monoenergetic beam by the pulse P_2. The range at which diffraction phenomena become predominant corresponds to $\Delta E_{\mathrm{Qu}} \geq \Delta E_{\mathrm{cl}}$, leading to $\tau \leq 50\ \mu$s.

The energy distribution after P_2 is determined by a time-of-flight technique, by measuring the number of atoms bouncing on a third pulse P_3, whose temporal position is scanned around $5T$. The width of P_3 is also τ, so that the broadening of the energy distribution in the measurement process remains small.

The major part of our experimental setup has been described elsewhere [6]. It consists of a double cell vacuum system, in which atoms are first captured in a MOT located in the upper part [7]. The Cs vapor pressure in the upper cell is relatively high (6×10^{-8} mbar) which allows us to capture $\sim 10^8$ atoms in 1 s. These atoms are released, and they fall into the lower cell, located 70 cm below, where the pressure is much lower (3×10^{-9} mbar). They are recaptured in a second MOT, located 3 mm above the

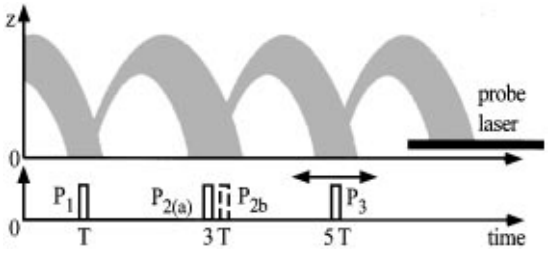

FIG. 1. A cold atomic cloud is released above a mirror formed by an evanescent laser wave. This mirror intensity I is chopped for two short pulses P_1 and P_2. The energy distribution is probed using a time-of-flight method, by measuring the number of atoms bouncing on a third pulse P_3 whose temporal position is scanned. By replacing P_2 by two pulses P_{2a} and P_{2b} (dashed line), we realize the temporal equivalent of a Young slit interferometer.

 0031-9007/96/77(1)/4(4)$10.00

dielectric prism used for the atomic mirror. The transfer efficiency is 20%, so that every 1.6 s, 2×10^7 atoms are released above the mirror, at a temperature $\sim 5\ \mu$K, in the $F = 4$ hyperfine ground state.

The prism surface is concave, with radius of curvature 2 cm. The evanescent wave (EW) has a circular Gaussian profile, with $1/e^2$ radius $w = 300\ \mu$m. It is formed using the total internal reflection of a laser with intensity $I = 100$ mW, with a linear polarization in the reflection plane; it is blue detuned by $\delta = 9.5$ GHz from the resonance line $6s_{1/2}$, $F = 4 \leftrightarrow 6p_{3/2}$, $F = 5$. The EW therefore creates a potential barrier along the z-vertical direction $U(x, y, z) \propto I \exp[-2(x^2 + y^2)/w^2] \exp(-2\kappa z)/\delta$, where $\kappa^{-1} = 0.19\ \mu$m is the decay length for the EW electric field. The EW mirror is switched on and off by an acousto-optic modulator used in the zeroth order, triggered by a quartz-stabilized function generator. The switching time is $\sim 0.5\ \mu$s, similar to the atomic bouncing time $1/\kappa v_i \sim 1\ \mu$s, where $v_i = gT$ is the incident velocity on the mirror. The extinction ratio is typically 1:10, while a reduction of the EW by a factor of 2 is sufficient to prevent the bouncing of atoms with energy E_0.

The number of atoms which can perform the sequence of three bounces of Fig. 1 varies as τ^2 in the classical region ($\tau > 50\ \mu$s) and as τ^3 in the quantum region, provided P_3 is centered on $5T$. In order to increase this number, one could increase the size of the reflecting disk, by increasing I or reducing δ. However, we preferred to keep a small mirror surface, since this provides an efficient way to eliminate atoms which bounce on an irregularity of the mirror surface. These irregularities, which can be due either to a defect in the polishing of the mirror or to a residual standing wave component in the evanescent field [8], cause a large horizontal-vertical coupling during the bounce. This changes the vertical kinetic energy of the atoms, and it causes a random change of the arrival time of the atoms on P_3.

To increase the number of atoms contributing to a given shot, we have replaced each individual pulse P_1, P_2, P_3 by a sequence of ~ 10 pulses (not shown in Fig. 1). The separation between two consecutive pulses within each of the three sequences ranges from 400 μs for $\tau \leq 40\ \mu$s, up to 1200 μs for $\tau = 100\ \mu$s; it is chosen large enough so that there is no overlap between the various patterns going through the time slits. The number of atoms per shot for $\tau = 40\ \mu$s is ~ 40 for the optimal position of the sequence of pulses P_3. In order to detect those atoms, we have measured the fluorescence induced by a weak resonant probe beam using a cooled photomultiplier. Each atom scatters $\sim 10^4$ photons, among which 10 are detected on average, due to the detection solid angle and to the photomultiplier sensitivity. The signal therefore constitutes in a bunch of $40 \times 10 = 400$ photons, distributed over the duration (4 ms) of the detection window. The stray light is responsible for a similar background signal (10^5 detected photons/s). We note that this detection scheme was possible thanks to the double cell system, which guarantees that the Cs vapor pressure is low in the prism region and that the resonant scattering from this vapor remains small enough.

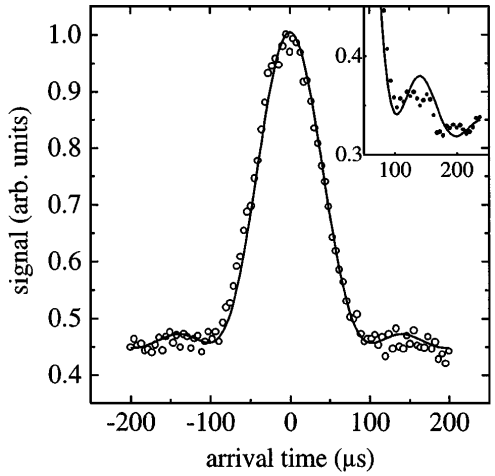

FIG. 2. Experimental time-of-flight signal for a pulse duration $\tau = 30\ \mu$s (circles); theoretical prediction (continuous curve) using the temporal version of the Huygens-Fresnel principle. Inset: magnification of the sideband signal.

A typical time-of-flight spectrum is represented in Fig. 2 for $\tau = 30\ \mu$s. It gives the fluorescence induced by the probe laser as the temporal position of P_3 is scanned. Each of the 90 points of this figure has been averaged 170 times so that the total acquisition time for such a plot is 7 h. We have repeated this experiment for various τ, and we have plotted in Fig. 3 the corresponding FWHM ΔT. For large τ, we find that ΔT increases with τ as expected from classical mechanics. When τ decreases, ΔT passes through a minimum and increases again, as expected from the time-energy uncertainty relation. The error bars shown in Fig. 3 indicate the statistical fluctuations of ΔT in a series of measurements.

This experiment requires a precise cancellation of the residual magnetic field. Indeed an atom may change its magnetic sublevel during the bounce, which converts a

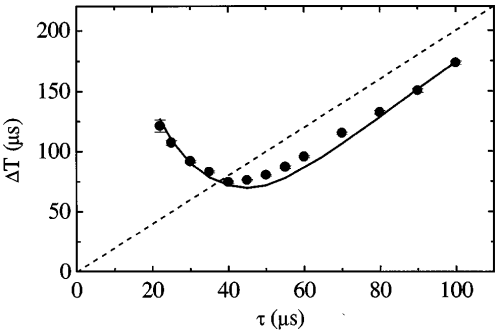

FIG. 3. Experimental (circles) and theoretical (continuous curve) FWHM ΔT of the time-of-flight signals, as a function of the pulse width τ. The dotted line is classical prediction $\Delta T = 2\tau$.

fraction of its kinetic energy into internal Zeeman energy [9]; the center of the corresponding diffraction peak is then displaced with respect to $5T$. In practice we require $B < 2$ mG so that the maximal shift of the arrival time $\sim T\mu_B B/E_0$, where μ_B is the Bohr magneton, remains small compared with the minimum time width appearing in Fig. 3, $\Delta T \sim 75\ \mu$s.

We have also plotted in Fig. 3 the result of a theoretical analysis based on the path integral approach, which is well suited for this Fresnel-like diffraction problem. The probability for having an atom bouncing during P_1 at time t_i and during P_3 at time t_f is given by

$$\mathcal{P}(t_i, t_f) = \left| \int A(t_i, t_r) A(t_r, t_f)\, dt_r \right|^2, \qquad (1)$$

where the integral over the intermediate bounce time t_r is taken inside P_2. In this temporal version of the Huygens-Fresnel principle, the quantity $A(t, t')$ is the propagator of a particle in the gravitational field [10]. We then integrate $\mathcal{P}(t_i, t_f)$ over the pulses P_1 and P_3. In this calculation, the widths of the pulses have been slightly corrected to account for the fact that atoms bouncing close to the time at which the mirror is switched *on* or *off* gain or lose energy during the bouncing process, and do not contribute to the peak represented in Fig. 2. The reduction of the time width is determined from a classical analysis, and remains in any case small compared to the width of the pulses themselves. For instance, for $\tau = 40\ \mu$s, this leads to a reduction of 1 μs for the first and third pulses, and 3 μs for the second pulse.

In addition to the existence of a minimum width ΔT, which is a direct consequence of the time-uncertainty relation, there are two other signatures of the temporal diffraction phenomenon in the set of data presented here. First, sidebands appear on the time-of-flight data of Fig. 2 (see, in particular, the inset, in which the data have been averaged 850 times and smoothed over every 3 consecutive data points). Because of the convolution of the signal with the detecting pulse P_3, they are not as visible as in spatial diffraction experiments (see, e.g., [11] for neutron diffraction). Second, for large τ, the width ΔT is found to be smaller by $\sim 10\ \mu$s than the classical prediction (broken line in Fig. 3). This originates from the temporal equivalent, on each side of P_2, of the well known edge diffraction phenomenon [12,13].

We have then designed a temporal Young slit interferometer by splitting P_2 into two pulses P_{2a} and P_{2b} separated by a variable duration τ'. This is an analog for de Broglie waves of the Sillitto-Wykes photon experiment [14,15]. The interference occurs between the paths P_1-P_{2a}-P_3 and P_1-P_{2b}-P_3, as in a Young double slit experiment [2]. Figure 4(a) presents the time-of-flight distribution obtained with $\tau' = 40\ \mu$s. The measured interference profile between the paths P_1-P_{2a}-P_3 and P_1-P_{2b}-P_3 is in good agreement with the one calculated

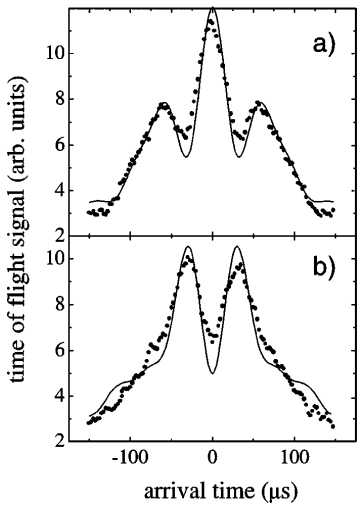

FIG. 4. Experimental (circles) and calculated (continuous curve) time-of-flight signals obtained in a temporal Young-slit configuration, in which the pulse P_2 is split into two pulses P_{2a} and P_{2b} separated by a duration $\tau' = 40\ \mu$s. (a) Equal mirror intensity for P_{2a} and P_{2b}; (b) phase shift of π between the two paths of the interferometer, obtained experimentally using a 3% reduction of the evanescent wave intensity during P_{2b}.

using the path integral approach, shown in a continuous line, which takes into account the finite width of the temporal slits. The experimental contrast is a bit lower than the predicted one, and we attribute this reduction to the residual magnetic field; for the fraction of atoms changing their magnetic sublevel during $P_{2a/b}$, as mentioned above, the velocity after the bounce is different from the incident one, and the corresponding interference pattern is slightly shifted.

The relative phase between the two arms of this interferometer can be easily scanned by changing the effective height of the mirror for P_{2b}, with respect to the mirror height for P_{2a}. This is done by changing the mirror intensity I by a quantity δI during the pulse P_{2b}, which displaces the atom turning point by

$$\delta z = (2\kappa)^{-1} \delta I / I\,, \qquad (2)$$

and modifies the path length of P_1-P_{2b}-P_3 by $2\delta z$. A phase shift of π between the two paths is obtained for $\delta z = \Lambda_{\mathrm{DB}}/4$, where $\Lambda_{\mathrm{DB}} = h/mgT = 12$ nm is the de Broglie wavelength of the atoms incident on the mirror. In our experimental condition, this corresponds to $\delta I/I = 0.03$. The interference profile obtained in this situation is shown in Fig. 4(b). As expected, the central fringe then corresponds to a destructive interference.

Finally, Fig. 5 gives the interference signal obtained with the detecting pulse P_3 set on the central fringe ($t = 5T$), when the intensity for P_{2b} is scanned. Several extrema are visible and each maximum corresponds to constructive interference which occurs when the turning point in P_{2b} is displaced by a multiple of $\Lambda_{\mathrm{DB}}/2$. The

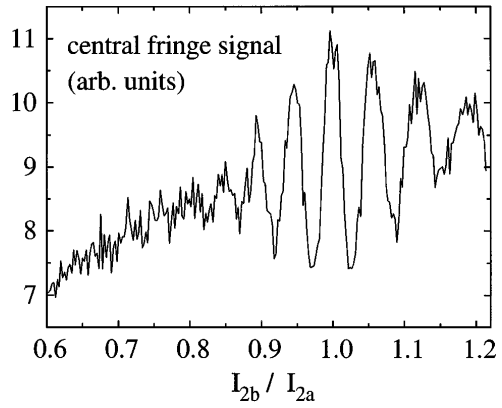

FIG. 5. Amplitude of the central fringe of the temporal Young-slit interferometer as a function of the evanescent wave intensity I_{2b} during the pulse P_{2b}. The intensity I_{2a} during the pulse P_{2a} is constant. The maxima correspond to a path difference between the two arms multiple of $\Lambda_{\mathrm{DB}}/2 = 6$ nm.

reduction of the contrast as δI increases is due to the van der Waals interaction between the bouncing atoms and the dielectric; this interaction modifies the simple prediction (2), so that the phase shift actually varies with the distance between the turning point of the atomic trajectory and the dielectric surface, and therefore depends on the atomic transverse position in the Gaussian evanescent wave.

This latter experiment can be used for a measurement of the van der Waals interaction, by analyzing precisely the variation of the phase difference between the two paths, as the turning point of P_{2b} gets closer to the dielectric. For a quantitative experiment, we will need a higher EW power than in the present experiment, so that all atoms bounce on a fraction of the mirror where the intensity is practically constant and turn at the same distance from the mirror. The number of visible oscillations should then be limited only to T/τ, because of the broadening $\Delta\Lambda_{\mathrm{DB}} \sim \Lambda_{\mathrm{DB}}\ \tau/T$ due to the temporal width τ of the source slit. Another application of this interferometer is a *Welcher Weg* experiment, using a nondestructive detection of the bouncing atoms [16].

To summarize, we have presented a quantitative test of the time-energy uncertainty principle by measuring the diffraction of atomic matter waves by a temporal slit. This is complementary to the diffraction of matter waves by a time periodic potential recently observed for neutrons [17] and for atoms [6]. We have also used the coherently diffracted atoms to design a temporal Young slit interferometer. In the context of atom optics, the observation of interferences in this trampoline geometry is important since it shows that the coherence of the de Broglie wave can be maintained over a bounce [18]. Therefore this is a significant step towards a coherent Fabry-Perot cavity for atomic waves using evanescent wave mirrors.

We thank C. Cohen-Tannoudji, C. Salomon, A. Steane, and P. Desbiolles for useful discussions. M. A. acknowledges financial support by the EEC through a Community training project and by the Alexander von Humbolt Foundation. This work is partially supported by DRET, CNRS, Collège de France, and DRED.

*Unité de Recherche de l'Ecole normale Supérieure et de l'Université Pierre et Marie Curie, associée au CNRS.

[1] M. Moshinski, Phys. Rev. **88**, 625 (1952); A. S. Gerasimov and M. V. Kazarnovskii, Sov. Phys. JETP **44**, 892 (1976); J. Felber, G. Müller, R. Gälher, and R. Golub, Physica (Amsterdam) **162B**, 191 (1990); A. Zeilinger and C. Brukner (to be published).

[2] O. Carnal and J. Mlynek, Phys. Rev. Lett. **66**, 2689 (1991); F. Shimizu, K. Shimizu, and H. Takuma, Phys. Rev. A **46**, R17 (1992).

[3] D. W. Keith *et al.*, Phys. Rev. Lett. **66**, 2693 (1991); E. Rasel *et al.*, Phys. Rev. Lett. **75**, 2633 (1995); D. M. Giltner, R. W. McGowan, and S. A. Lee, Phys. Rev. Lett. **75**, 2638 (1995).

[4] C. Bordé, Phys. Lett. A **140**, 10 (1989); F. Riehle *et al.*, Phys. Rev. Lett. **67**, 177 (1991); M. Kasevich and S. Chu, Phys. Rev. Lett. **67**, 181 (1991); Ch. Miniatura *et al.*, Phys. Rev. Lett. **69**, 261 (1992); K. Sengstock *et al.*, Appl. Phys. B **59**, 99 (1994).

[5] R. J. Cook and R. K. Hill, Opt. Commun. **43**, 258 (1982).

[6] A. Steane, P. Szriftgiser, P. Desbiolles, and J. Dalibard, Phys. Rev. Lett. **74**, 4972 (1995).

[7] C. Monroe, W. Swann, H. Robinson, and C. Wieman, Phys. Rev. Lett. **65**, 1571 (1990).

[8] C. Westbrook and A. Aspect (private communication).

[9] R. Deutschmann, W. Ertmer, and H. Wallis, Phys. Rev. A **48**, R4023 (1993).

[10] R. P. Feynman and A. R. Hibbs, *Quantum Mechanics and Path Integrals* (McGraw-Hill, New York, 1965), p. 62.

[11] R. Gähler and A. Zeilinger, Am. J. Phys. **59**, 316 (1991).

[12] M. Born and E. Wolf, *Principles of Optics* (Pergamon, New York, 1980), 6th ed., p. 433.

[13] The reduction of the pulse width, due to the large increase or decrease of energy of the atoms as they bounce close to the edges of the pulses, has a negligible contribution in this range of values for τ.

[14] R. M. Sillitto and C. Wykes, Phys. Lett. **39A**, 333 (1972).

[15] The extension of [14] to neutrons has been discussed theoretically in H. R. Brown *et al.*, Phys. Lett. A **163**, 21 (1992).

[16] J.-Y. Courtois, J.-M. Courty, and S. Reynaud, Phys. Rev. A **52**, 1507 (1995); A. Aspect *et al.*, Phys. Rev. A **52**, 4704 (1995).

[17] J. Felber, R. Gähler, C. Rausch, and R. Golub, Phys. Rev. A **53**, 319 (1996).

[18] Long *internal* atomic coherence times have been observed in a trampoline geometry by N. R. Davidson *et al.*, Phys. Rev. Lett. **74**, 1311 (1995).